Computers Math. Applic. Vol. 18, No. 1–3, pp. 1–14, 1989
Printed in Great Britain

0097-4943/89 $3.00 + 0.00
Pergamon Press plc

FIGHTER EVASIVE BOUNDARIES AGAINST MISSILES

F. IMADO[1] and S. MIWA[2]

[1]Mechanical Systems and Technology Department, Central Research Laboratory, Mitsubishi Electric Corporation, Amagasaki, Hyogo, Japan

[2]Department of Electrical Communication Engineering, Faculty of Engineering, Tokyo Denki University, Tokyo, Japan

Abstract—The evasive boundaries of two types of fighters which have different g performances, against a proportional navigation guidance missile and an augmented proportional navigation guidance missile are studied. The fighters are supposed to take different evasive maneuvers such as sustained maximum g turn, high-g barrel roll and optimal evasive maneuvers. Studies are made for the combination of above fighters and missiles in several altitudes. The results show that the fighter evasive region is more restricted against an augmented proportional navigation missile than a proportional navigation missile particularly in high altitudes, and the high-g barrel roll is quite effective for both types of fighters. The interesting features are that the fighter can achieve a larger miss distance against an augmented proportional navigation missile if it takes an optimal evasive maneuver.

NOMENCLATURE

a = Lateral acceleration
a_c = Missile lateral acceleration command signal
C_D, C_L = Drag and lift coefficients, respectively
C_{D0} = Zero-lift drag coefficient
D = Drag
g = Acceleration of gravity
h = Altitude
J = Performance index
k = Induced drag coefficient of aircraft
k_1, k_2 = Drag coefficients of missile
L = Lift
m = Mass
M = Mach number
N_e = Effective navigation constant
r = Slant range between missile and aircraft
s = Reference area
t = Time
t_e = Sustainer burning time
t_f = Interception time
t_{go} = Time-to-go
T = Thrust
v = Velocity
v_c = Closing velocity
x = Horizontal coordinate
α, α_0 = Angle-of-attack and zero-lift angle
θ = Angles in Fig. 1b
ρ = Air density
σ, γ = Line-of-sight and flight-path angles, respectively
τ = Missile time constant
Ω = Terminal condition
$(\cdot)$ = Time derivative

Subscripts

a = Aircraft
c = Command or corner
0, f = Initial and terminal values, respectively
m = Missile
max, min = Maximum and minimum values, respectively

INTRODUCTION

The authors have studied the fighter (hereafter called "aircraft") evasive maneuvers such as the optimal evasive maneuvers [1], the maximum sustained g turns and their delayed effect [2], and the high-g barrel rolls (HGB) [3]. However, these studies were done against a proportional navigation (PNG) missile. As is said, the augmented proportional navigation guidance (APNG) [4] seems promising in near future. The essential idea of APNG is to introduce a target acceleration compensation term into PNG. Therefore provided with the information on the target acceleration (usually estimated by a Kalman filter), its application to a current PNG missile is straightforward. It may be instructive to study the evasive regions against an APNG missile and to compare with the results against a PNG one.

This paper studies on evasive boundaries of two types of fighters (one is a conventional and the other is an advanced) against two kinds of missiles (one is navigated by the PNG law and the other, by APNG).

General purpose tactical missile simulation program (GPMS) [5] which provides with fairly precise mathematical models, is used in the simulation studies. As for aircraft optimal evasive maneuvers, the steepest ascent method [6, 7] is employed in order to solve nonlinear two point boundary value problems.

The mathematical principle of PNG and APNG is introduced first. Then, the simulation models of aircrafts and missiles are explained. The simulation results on the evasive boundaries achieved by sustained maximum g turns and high-g barrel roll maneuvers are shown. Finally, some features of optimal maneuvers against PNG and APNG missiles are shown.

THE PRINCIPLE OF PNG AND APNG

Figure 1a shows a two-dimensional geometry of a missile and an aircraft. When both vehicles fly in a collision course, the line-of-sight angle σ is retained constant and they will intercept at a position P. Whereas in the case the aircraft accelerates longitudinally or laterally, the value of σ varies. The idea of PNG is to change the missile course with the lateral acceleration a_m which is proportional to the time change rate of σ ; $\dot{\sigma}$. Then both vehicles enter into the new collision courses which intercept at P'. The mathematical principle of the PNG is as follows.

Let us consider a simple intercept problem to find $a(t)$ which minimize J:

$$\dot{v} = a(t); \tag{1}$$

$$\dot{y} = v; \tag{2}$$

$$J = \tfrac{1}{2}cy_f^2 + \frac{1}{2}\int_t^{t_f} a^2(t)\,dt. \tag{3}$$

The solution is easily obtained [8] by the linear optimal control theory:

$$a(t) = \frac{-(t_f - t)^2 v(t) - (t_f - t)y(t)}{\dfrac{1}{c} + \tfrac{1}{3}(t_f - t)^3}. \tag{4}$$

If $c \to \infty$, then y_f in equation (3) reduces to zero, and

$$a(t) = -3\left(\frac{v(t)}{t_f - t} + \frac{y(t)}{(t_f - t)^2}\right). \tag{5}$$

Figure 1b shows a simplified geometry and symbols of PNG. If we translate symbols from equations (6)–(8), this figure becomes equivalent to the problem expressed by equations (1)–(3):

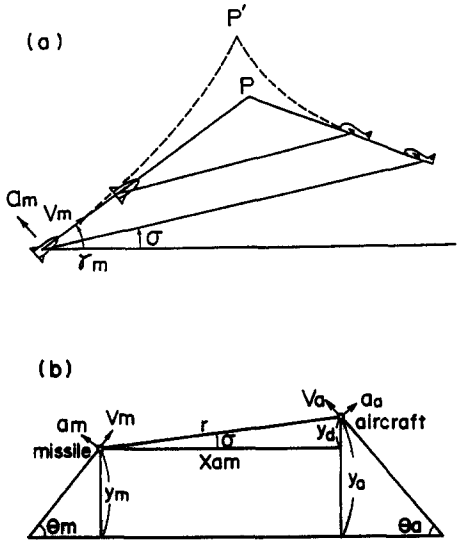

Fig. 1. The conception of proportional navigation guidance. (a) Collision triangle; (b) simplified geometry.

$$y = y_m - y_a = -y_d; \tag{6}$$

$$v = v_m \sin\theta_m - v_a \sin\theta_a = -v_d; \tag{7}$$

$$a = a_m \cos\theta_m - a_a \cos\theta_a. \tag{8}$$

Let v_c = closing velocity along the line-of-sight, and let

$$\sigma \approx \frac{-y(t)}{v_c(t_f - t)}. \tag{9}$$

Then

$$a = 3v_c\dot{\sigma}. \tag{10}$$

The ordinary PNG law is

$$a_m = N_e v_c \dot{\sigma}, \tag{11}$$

where N_e is the effective navigation constant. If we set N_e to be 3, and θ_m, θ_a be small, then we find equation (11) is the solution to minimize

$$\int_t^{t_f} a_m^2(t)\,dt$$

for a nonmaneuvering aircraft ($a_a = 0$ means $a_m = a$) with final miss distance y_f to be zero.

Now we replace $t_f - t$ in equation (5) by t_{go}, then we obtain

$$a_m(t) = \frac{N_e}{t_{go}^2}(y_d + v_d t_{go}). \tag{12}$$

The value of the parentheses in the right-hand side of equation (12) is the predicted miss distance at t_f when the missile does not accelerate. In the case the missile knows the aircraft acceleration a_a, the guidance law may be improved by introducing the miss distance derived by a_a into equation (12). Then we get

$$a_m(t) = \frac{N_e}{t_{go}^2}(y_d + v_d t_{go} + \tfrac{1}{2}a_a t_{go}^2). \tag{13}$$

This guidance law is called APNG [4]. The same guidance law is also obtained as a special case of the optimal guidance laws for accelerating targets solved by Garver [9]. Equation (13) is equivalently rewritten as

$$a_m(t) = N_e(v_c\dot{\sigma} + \tfrac{1}{2}a_a). \tag{14}$$

The guidance law has the same advantage as PNG in not requesting the information about t_{go}. Therefore the hardware mechanization is simple if the missile can estimate the aircraft acceleration by an extended Kalman filter or other techniques. A simulation example of the miss distance by a PNG and an APNG missile is shown in Fig. 2. The abscissa is the time when the aircraft

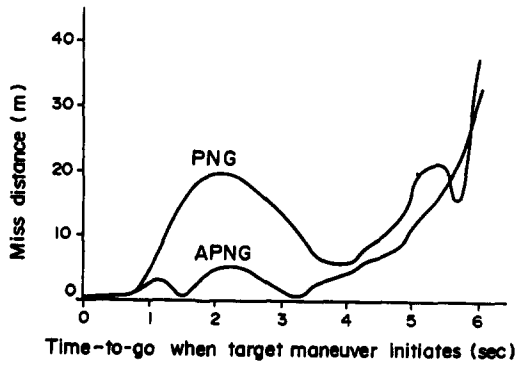

Fig. 2. Miss distance by PNG and APNG ($v_0 = 600$ m/s, $h_0 = 3000$ m, $r_0 = 5000$ m).

(conventional one, which will be explained in the next section) initiates the sustained maximum g turn. The initial relative range is 5 km, the initial missile and aircraft velocities are 600 and 300 m/s respectively, and the altitudes are both in 3000 m. Imado and Miwa [1] showed that miss distance becomes large when an aircraft initiates a sustained maximum g turn (or a split-S) one or two seconds before interception. This is true for the PNG missile as shown in Fig. 2, but for the APNG missile, miss distance is small compared with the PNG missile. The reason is naturally thought as the predicting effect of the term in equation (14).

AIRCRAFT AND MISSILE MODELS

The different mathematical models of the aircraft and missiles are employed in the simulation study of the evasive boundaries and in the miss distance calculation of optimal evasive maneuvers. In the former study, a conceptual medium range air-to-air missile is considered where the fairly precise missile dynamics and the guidance loop mathematical models are provided. However, rather simple constant velocity point with a lateral acceleration model is employed for the aircraft. The prime reason is due to the fact that, the thrust, weight, wing area and aerodynamic coefficients etc. are different from aircraft to aircraft, but the most important factor for missile avoidance at the final homing phase is their available side-gs.

Therefore a conventional aircraft and a rather advanced one are distinguished by the different side-gs. Whereas in the latter study, nonlinear two point boundary value problems (NTPBVP) must be solved numerically to obtain the aircraft angle-of-attack α (or equivalently lift coefficient C_L) and the thrust histories under reasonable aerodynamic constraints. Point mass models [1, 2] are employed for both vehicles which provide with fairly precise dynamic features of vehicles within the ability of computer to solve NTPBVP. More detailed explanation will be delivered in the later section. Although the simulation models are different, the main features are kept the same.

Figure 3 shows the available side-gs of the assumed aircraft. Aircraft A has a 7 g performance at sea level, whereas aircraft B has a more than 9 g performance at a lower altitude of less than 3000 m. The maximum g is limited to 9 g considering the pilot endurance.

Figure 4 shows the relation between the velocity of the missile and its available side-gs. Although the missile may have more ability, the acceleration command signal is limited to 30 g in the pitch and yaw axes in order to prevent excessive velocity reduction. In the middle of these two axes, a more than 40 g performance is available. The drag parameters k_1 and k_2 appearing in the next section are shown in Fig. 5. They correspond to the missile parasite drag and the induced drag respectively. Other parameters are almost equivalent to the values appearing in the following sections.

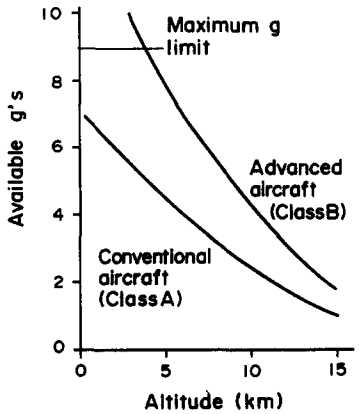

Fig. 3. The available g performance of the aircraft.

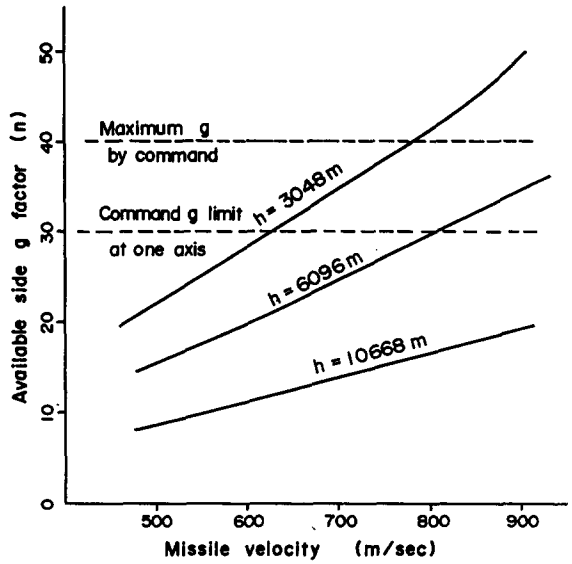

Fig. 4. Missile velocity vs available g.

EVASIVE BOUNDARIES BY SUSTAINED MAXIMUM g TURNS

In this section, aircraft evasive boundaries by sustained maximum g turns (SMGT) are shown. Imado and Miwa [1] showed that a downward maneuver, which makes the best use of gravity, is more advantageous than a horizontal or upward one. But the aircraft may have not enough time to nose up in low altitudes. Therefore the aircraft is supposed to take a horizontal SMGT at altitudes less than 10,000 m, and a more advantageous downward SMGT (split-S) at altitudes more than 10,000 m where the aircraft easily can nose up again. In the simulation study, 1.0 g of gravity is added to the aircraft g performance shown in Fig. 4 for altitudes of more than 10,000 m. At the initial time, missiles are supposed to be in their coasting phase and lie in the collision course with flight path angles of 0–45°. The initial slant range between a missile and an aircraft is set to about 3–6 km. Figure 6 shows the evasive boundaries of aircraft A with SMGT maneuvers, where the

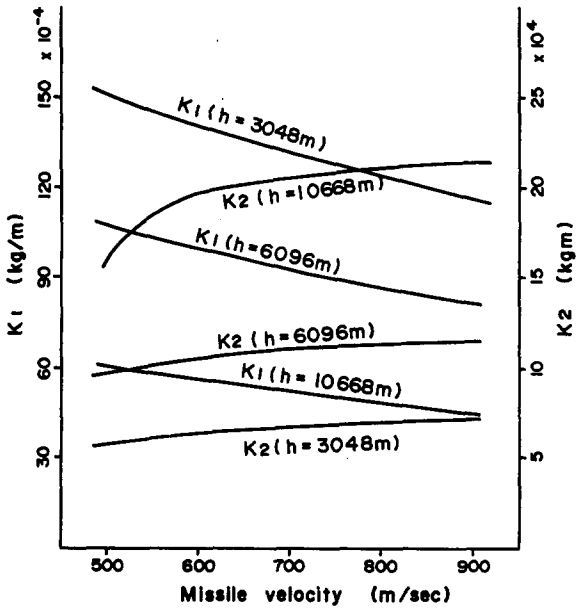

Fig. 5. Missile velocity vs drag parameters k_1 and k_2.

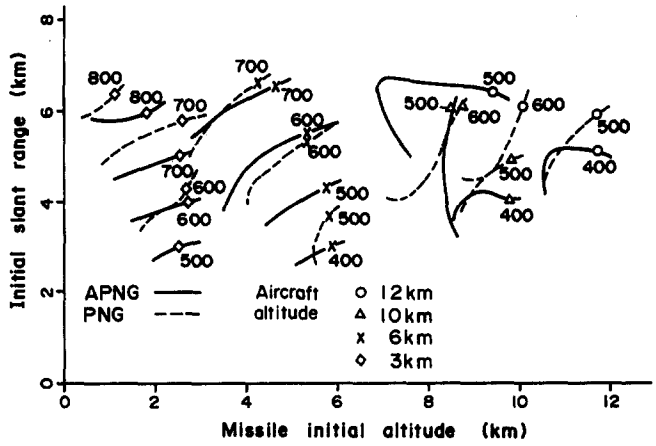

Fig. 6. The evasive boundaries of aircraft A with SMGT.

abscissa is missile initial altitude, and the ordinate is initial slant range. At the initial time, the aircraft and the missile are assumed to be on a collision course and the aircraft is assumed to take an instantaneous SMGT maneuver downward vertical or right-hand side horizontal. The dashed lines and bold lines show where miss distances become 10 m against PNG and APNG missiles respectively. The symbols and numbers show the corresponding aircraft altitude and the missile initial velocities (m/s) respectively. Against the missile outside (farther) of those boundary lines, the aircraft evasive maneuver becomes successful. Other boundaries may exist in inner region where the initial slant range is less than 3 km (which is not studied here because of the assumed scenario), where miss distance becomes large because of the lack of missile navigation time. Figure 6 shows that the missiles require higher speed in a low altitude than in a high altitude. The reason is easily understood from Figs 3 and 4 that the degradation of the aircraft g performance at the higher altitude is greater than that of the missiles. Figure 6 also shows that the missile velocities must be larger for a longer initial slant range and for a larger flight path angle. These are understood from the view point of the kinetic energy necessary for the missile.

Figure 7 shows the evasive boundaries of aircraft B with SMGT maneuvers. It is apparent that the missiles require larger velocities against aircraft B than against aircraft A in order to obtain the boundaries of the same distance. The PNG missiles need larger velocities than the APNG ones for both aircraft, and the tendency is clear at high altitudes. The reason is explained as follows. Generally speaking, the lateral acceleration command of a PNG missile rapidly rises up only in the neighborhood of interception where the change of the missile–aircraft geometry produces the large line-of-sight rate $\dot{\sigma}$. However, in order to respond this high side-g command, very large velocities are required for the PNG missile at a high altitude. On the other hand, for an APNG

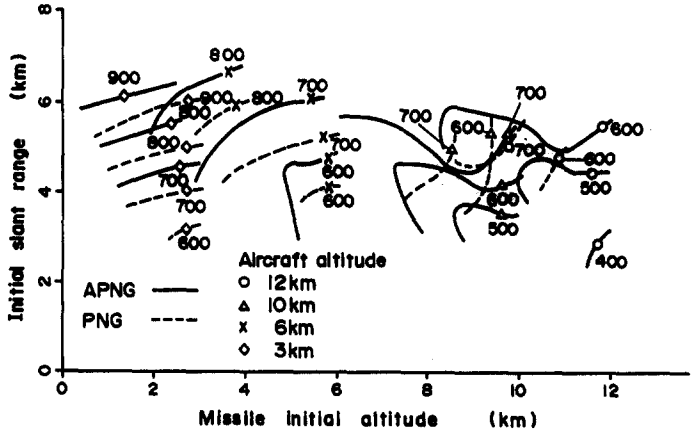

Fig. 7. The evasive boundaries of aircraft B with SMGT.

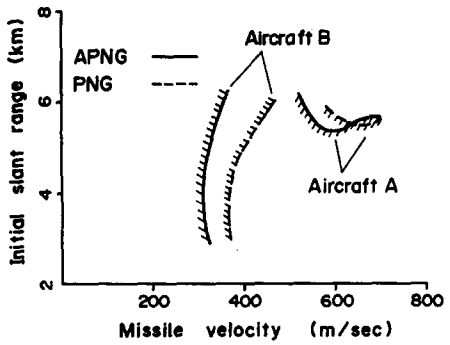

Fig. 8. The inner evasive boundaries vs missile velocities at 15,000 m altitude.

missile, the aircraft lateral acceleration is detected and the missile trajectory is gradually changed in earlier times. Thus the missile side-g command tends to be small, and a large velocity is not required. Another good example to explain this fact is Fig. 8, where the inner evasive boundaries at the altitude of 15,000 m are shown. The abscissa is the missile velocity, the ordinate is the missile aircraft initial slant range. The hatched regions outside the dashed or bold lines show where the miss distances become larger than 10 m against PNG and APNG missiles respectively. At the altitude of 15,000 m where the air density is very low, the velocity demand is more stringent for the PNG missile than for the APNG one. In other words, the minimum slant range necessary for navigation becomes larger for the PNG missile.

EVASIVE BOUNDARIES BY HIGH-g BARREL ROLL MANEUVERS

In this section, the aircraft evasive boundaries by high-g barrel roll (HGB) maneuvers are shown. Imado and Miwa [2] showed that HGB maneuvers produce far larger miss distances than SMGT, they are even comparable to that of two-dimensional optimal evasive maneuvers. In the SMGT, the miss distance changes greatly in relation to the maneuver initiation time as is seen in Fig. 2. This maneuver is relying on the transient response of a missile single axis guidance loop. On the other hand, HGB seems to be making use of the stationary resonance of a missile pitch–yaw guidance loop. An aircraft always can bring about a large miss distance, if it starts HGB of 1.5–2 rad/s roll rate more than 3 s before interception. The maneuver is far easier for a pilot to implement than the optimal maneuver in the following section, but it may not be so easy as SMGT. Therefore only 80% of the aircraft maximum side-g performance is assumed to be available in HGB. Although the miss distances become generally large, the conventional aircraft is still intercepted in the small restricted areas. Figures 9 and 10 show the evasive boundaries of

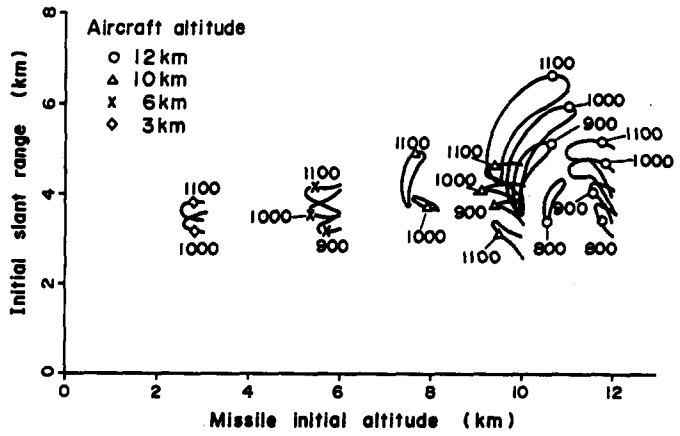

Fig. 9. The evasive boundaries of aircraft A with HGB against a PNG missile.

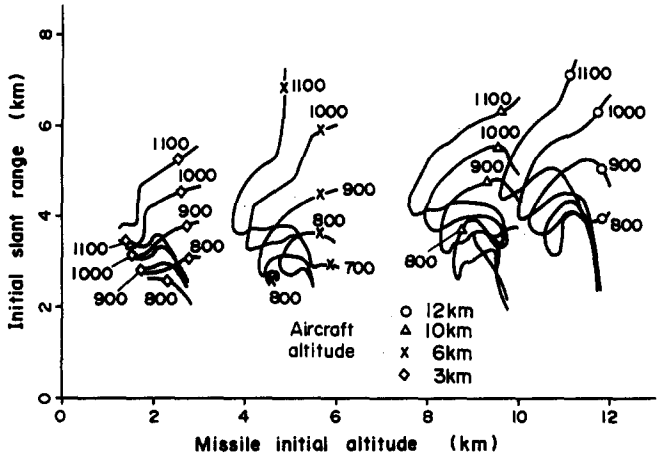

Fig. 10. The evasive boundaries of aircraft A with HGB against an APNG missile.

aircraft A with 1.5 rad/s HGB against a PNG and an APNG missile respectively. The bold lines show where the miss distance becomes 10 m, and the symbols and numbers have the same meanings as in Figs 6 and 7. Outside the fully enclosed contours or the open contours (open contours will make enclosed contours if overall simulation is done), the HGB maneuvers are successful. Against a PNG missile, the hit regions (where the miss distance becomes less than 10 m) are very small and differs according to the missile velocity. Against an APNG missile, the hit regions become wider but still are restricted to the small regions. The advanced aircraft B can almost always evade from a PNG missile with HGB, therefore the hit region is not illustrated here. Figure 11 shows evasive boundaries of aircraft B with HGB, against an APNG missile. The evasive regions are far wider compared with aircraft A. Referring to these figures, we may say HGB is a superior maneuver than SMGT for an aircraft.

OPTIMAL EVASIVE MANEUVERS

Intensive studies have been performed on the two-dimensional optimal evasive maneuvers of an aircraft against a PNG missile, but there seems no paper has ever dealt with APNG. As APNG seems to be one of the most promising missile guidance laws, there will be of some interest to compare the optimal strategies of a fighter against these two laws. Point mass models are employed for both a missile and an aircraft, which neglect rigid body rotation but still provide with the fairly precise kinematics of translation.

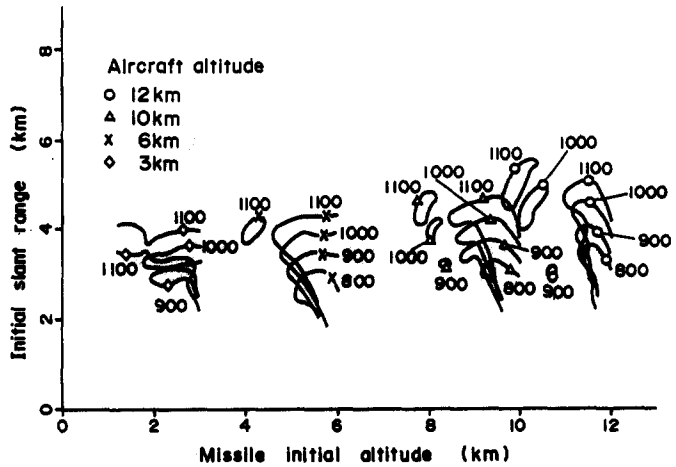

Fig. 11. The evasive boundaries of aircraft B with HGB against an APNG missile.

AIRCRAFT MOTION

The study is performed in the vertical plane. The equations of motion are shown by

$$\dot{v}_a = \frac{T}{m_a}\cos\alpha - \frac{D}{m_a} - g\sin\gamma_a; \tag{15}$$

$$\dot{\gamma}_a = \frac{L}{m_a v_a} + \frac{T}{m_a v_a}\sin\alpha - \frac{g}{v_a}\cos\gamma_a; \tag{16}$$

$$\dot{h}_a = v_a \sin\gamma_a; \tag{17}$$

$$\dot{x}_a = v_a \cos\gamma_a, \tag{18}$$

and

$$L = \tfrac{1}{2}\rho v_a^2 s_a C_L; \quad C_L = C_{L\alpha}(\alpha - \alpha_0); \tag{19}$$

$$D = \tfrac{1}{2}\rho v_a^2 s_a C_L; \quad C_D = C_{D0} + kC_L^2. \tag{20}$$

In order to eliminate to introduce any state constraints, $C_{L\alpha}$ is reduced when v_a exceeds the corner velocity v_{ac}:

$$C_{L\alpha} = \begin{cases} C_{L\alpha 0} & \text{for} \quad v_a \leqslant v_{ac}; \\ C_{L\alpha 0}\left(\dfrac{v_{ac}}{v_a}\right)^2 & \text{for} \quad v_a > v_{ac}. \end{cases} \tag{21}$$

MISSILE MOTION

The missile lateral acceleration is approximated by a first order lag to a lateral acceleration command. For simplicity, the missile mass is assumed constant. The control laws are assumed to be a constant gain PNG or APNG with the signal saturation taken into consideration, thus

$$\dot{v}_m = (T_m - D_m)/m_m; \tag{22}$$

$$\dot{a}_m = (a_c - a_m)/\tau; \tag{23}$$

$$\dot{\gamma}_m = a_m/v_m; \tag{24}$$

$$\dot{h}_m = v_m \sin\gamma_m; \tag{25}$$

$$\dot{x}_m = -v_m \cos\gamma_m, \tag{26}$$

where

$$D_m = k_1 v_m^2 + k_2(a_m/v_m)^2, \tag{27}$$

$$T_m(t) = \begin{cases} T_m & \text{for} \quad 0 \leqslant t \leqslant t_e, \\ 0 & \text{for} \quad t_e < t. \end{cases} \tag{28}$$

The acceleration command a_c is given for a PNG missile

$$a_c = \begin{cases} N_e v_c \dot{\sigma} & \text{for} \quad |a_c| \leqslant a_{cmax}, \\ a_{cmax}\,\text{sign}(a_c) & \text{for} \quad |a_c| > a_{cmax}, \end{cases} \tag{29}$$

or for an APNG missile

$$a_c = \begin{cases} N_e(v_c\dot{\sigma} + \frac{1}{2}a_a) & \text{for} \quad |a_c| \leqslant a_{cmax}, \\ a_{cmax}\,\text{sign}(a_c) & \text{for} \quad |a_c| > a_{cmax}, \end{cases} \tag{30}$$

where a_a is given by

$$a_a = v_a\dot{\gamma}_t. \tag{31}$$

In equations (29) and (30), N_e is the effective navigation constant, v_c the closing velocity, and $\dot{\sigma}$ the line-of-sight turning rate given by

$$v_c = -\dot{r}; \tag{32}$$

$$\dot{\sigma} = 1/r^2[(h_a - h_m)(\dot{x}_a - \dot{x}_m) - (\dot{h}_a - \dot{h}_m)(x_a - x_m)], \tag{33}$$

where r is slant range,

$$r = [(x_a - x_m)^2 + (h_a - h_m)^2]^{1/2}. \tag{34}$$

The performance index is the square of the terminal miss

$$J = [(x_a - x_m)^2 + (h_a - h_m)^2]_{t_f} \tag{35}$$

where interception time t_f is derived from the minimum range condition

$$\Omega = (x_a - x_m)(\dot{x}_a - \dot{x}_m) + (h_a - h_m)(\dot{h}_a - \dot{h}_m) = 0 \tag{36}$$

J in equation (35) is maximized by the steepest ascent method, in relation to two control parameters, viz. the aircraft angle-of-attack $\alpha(t)$ and thrust $T(t)$ under the following control constraints:

$$\alpha_{min} \leqslant \alpha \leqslant \alpha_{max}; \tag{37}$$

$$0 \leqslant T \leqslant T_{max}. \tag{38}$$

A negative α is interpreted as a positive $|\alpha|$ with 180° roll angle. No time lag is assumed for the α and T control, and the roll time constant is also neglected. The aircraft data are mainly derived from Heffley and Jewell [10] and Gilbert *et al.* [11] with minor modifications. The missile is in its sustainer phase with 8 s fuel left. Initial geometry is head-on in co-altitude with about 5 s time-to-go. The vehicle side-g performance and drag parameters are shown in Figs 4 and 5. Other parameters are shown in Table 1.

The miss distances by the optimal evasive maneuver for the combination of aircraft A and B, PNG and APNG missiles are shown in Figs 12 and 13. The figures include both cases, viz. the case where the missile lateral acceleration exceeds 30 g, and the case where its value is limited to 30 g. The miss distances are smaller at higher altitudes and for larger missile velocities, which are same as in the case of SMGT. But for the missiles having the 30 g limit, the miss distances become

Table 1. Parameters

	Aircraft A		Aircraft B	
m_a	17,656 kg		7500 kg	
S_a	49.24 m^2		26.00 m^2	
v_{a0}	290.0 m/s		290.0 m/s	
(h = 3048 m)				
C_{Lmax}	0.518		0.662	
C_{D0}	0.0165		0.0165	
k	0.150		0.150	
a_{amax}	5.6 g	(sustained)	9.0 g	(sustained)
T_{max}	199,600 N	(afterburner)	99,300 N	(afterburner)
(h = 10,668 m)				
C_{Lmax}	0.485		0.706	
C_{D0}	0.0261		0.0261	
k	0.167		0.167	
a_{amax}	2.2 g	(sustained)	4.0 g	(sustained)
T_{max}	94,400 N	(afterburner)	47,000 N	(afterburner)
Missile:				
m_m	200 kg			
T_m	6000 N			
t_c	8.0 s			
N_c	4			
τ	0.5 s			
a_{cmax}	See Fig. 4			
k_1, k_2	See Fig. 5			

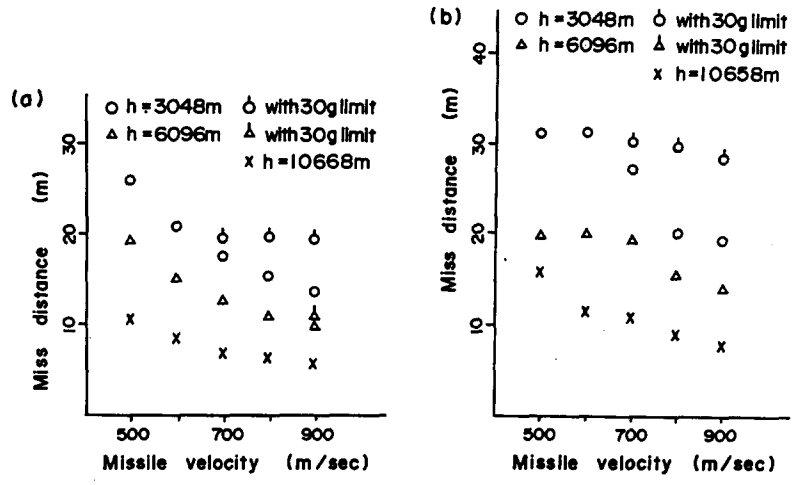

Fig. 12. Miss distances by aircraft A with optimal maneuvers vs missile velocities. (a) Against a PNG missile; (b) against an APNG missile.

constant if the missile velocities exceed a certain value. Therefore the prime factor on the miss distance is not the velocities but the available side-g of missiles.

The most prominent features of these figures are the fact that the optimal evasive maneuver brings about the larger miss distances against an APNG missile than a PNG missile. Figures 14a,b and 15a,b show the aircraft control histories against a PNG and an APNG missile which have the velocity of 700 m/s at the altitude of 3048 m with unlimited lateral acceleration. In the APNG cases, the controls changes are more rapid and frequent than in the PNG cases, and the large α change often occurs just before interception. This is explained that an aircraft acceleration is detected in earlier time by an APNG missile, therefore the aircraft has to bring about a large acceleration change just before the interception. Figure 15c shows the case where missile lateral acceleration is limited to 30 g and the difference corresponds to the case of Fig. 15a. The aircraft does not change the α pattern, but it reduces the thrust level and decreases its velocity. Figure 16a is the case where the missile velocity is reduced to 500 m/s and corresponds to the case of Fig. 15b. It seems that the aircraft change controls more frequently against a high speed missile than a low speed one. Figures 16b and 16c show the case of aircraft B in high altitude of 10,668 m, against the APNG missile with velocities 500 and 900 m/s, respectively. The aircraft control histories are not largely affected by altitude except for the miss distances.

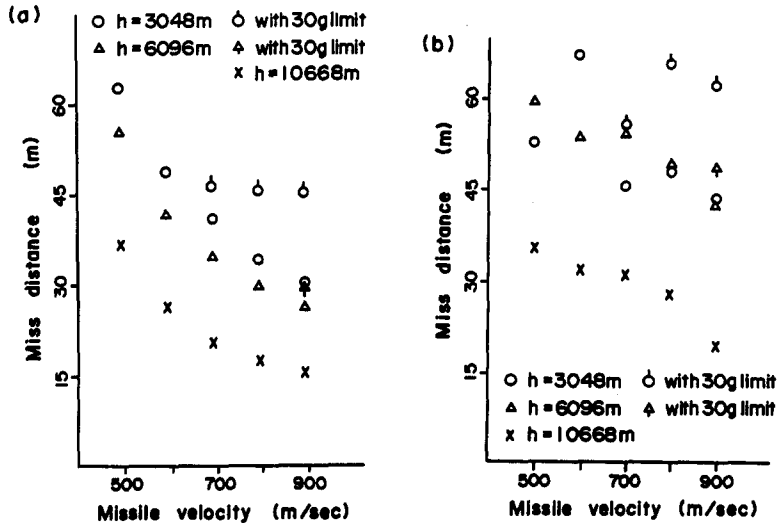

Fig. 13. Miss distances by aircraft B with optimal maneuvers vs missile velocities. (a) Against a PNG missile; (b) against an APNG missile.

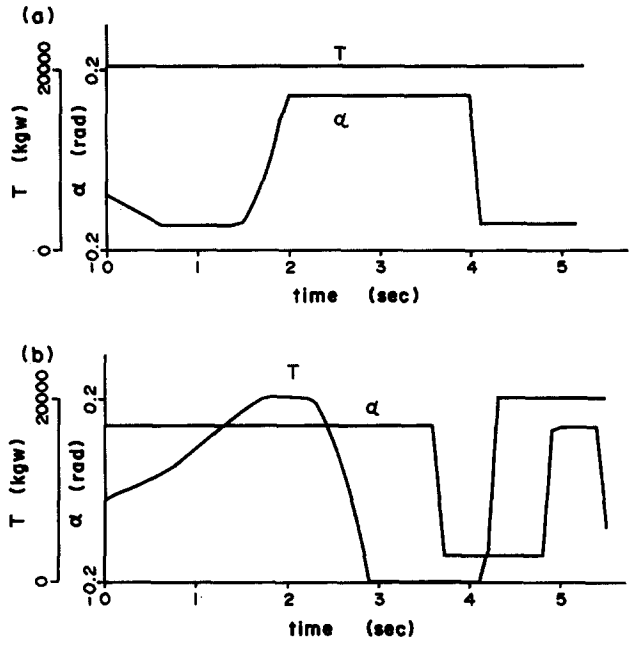

Fig. 14. The optimal control histories of aircraft A ($h = 3048$ m, $v_{m0} = 700$ m/s): (a) against a PNG missile; (b) against an APNG missile.

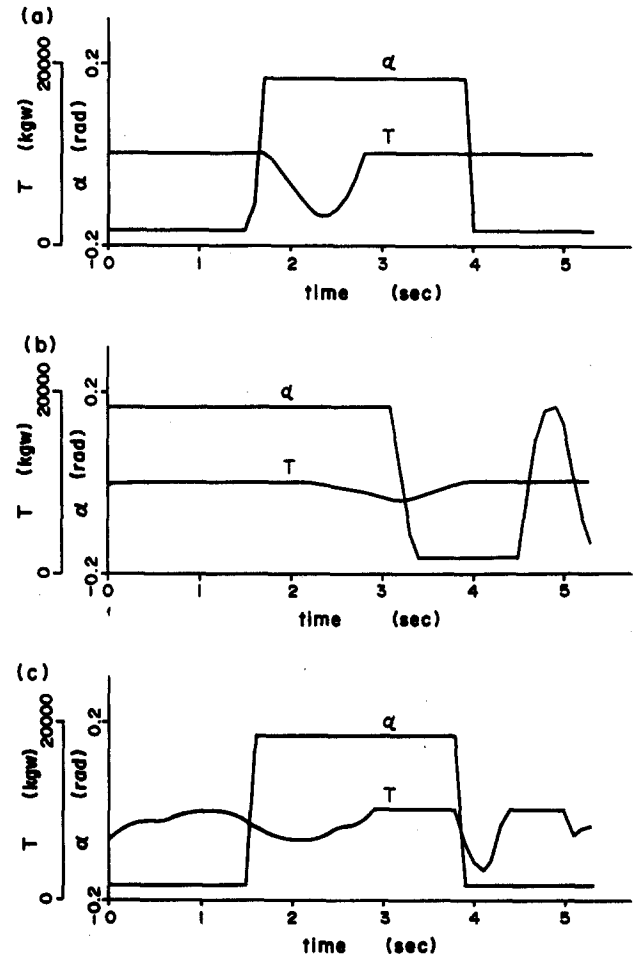

Fig. 15. The optimal control histories of aircraft B ($h = 3048$ m, $v_{m0} = 700$ m/s): (a) against a PNG missile; (b) against an APNG missile; (c) against a PNG missile with 30 g limit.

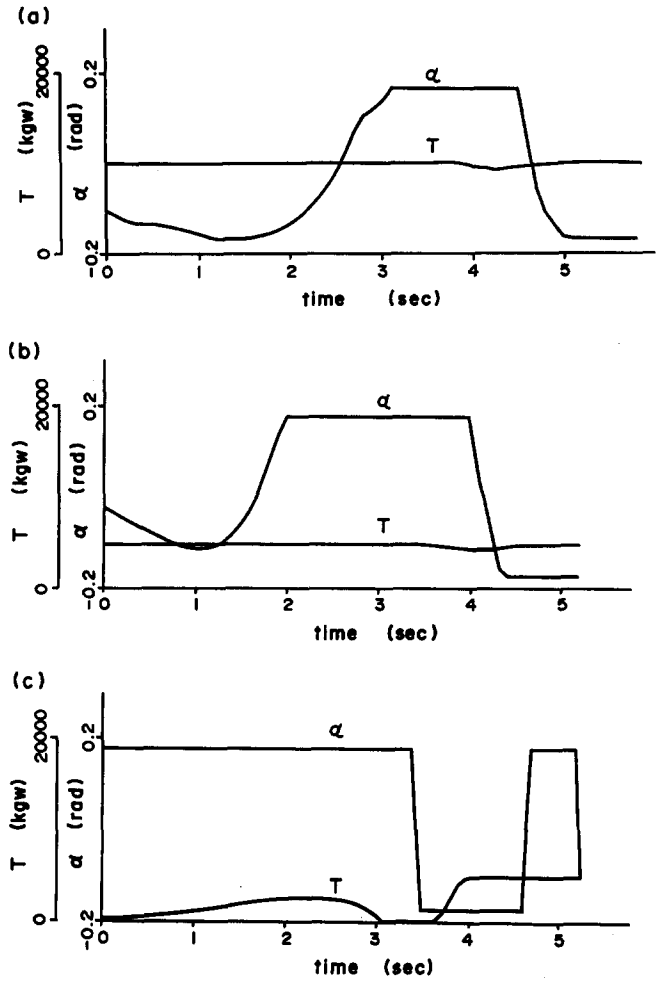

Fig. 16. The optimal control histories of aircraft B against an APNG missile: (a) $h = 3048$ m, $v_{m0} = 500$ m/s; (b) $h = 10{,}668$ m, $v_{m0} = 900$ m/s; (c) $h = 10{,}668$ m, $v_{m0} = 500$ m/s.

CONCLUSIONS

The evasive boundaries of two types of fighters, viz. a conventional and an advanced, against two types of missiles, viz. a proportional navigation and an augmented proportional navigation are studied. The simulation results show that if the aircraft takes sustained maximum g turns, the evasive region becomes narrower against an augmented proportional navigation missile than against a proportional navigation one, and this is particularly true at high altitudes, where the air density is low. Naturally, the advanced aircraft can extend the evasive region compared with the conventional aircraft.

The high-g barrel roll maneuver is very efficient for both types of aircraft. Although evasive and hit regions exist for the conventional aircraft against the augmented proportional navigation missile, the evasive region is largely extended against the proportional navigation missile. The advanced aircraft has a wider evasive region than the conventional aircraft against the augmented proportional navigation missile, and it can almost perfectly evade from the proportional navigation one.

The aircraft optimal evasive controls against the proportional navigation and augmented proportional navigation missiles are calculated in regard to angle of attack $\alpha(t)$ and thrust $T(t)$. It was found that the control histories are generally very different between the proportional navigation and the augmented proportional navigation missiles. These controls change more rapidly and frequently in against an augmented proportional navigation missile than a proportional navigation one. Large control changes often occur just before interception in against augmented proportional navigation missiles.

The prominent features of the optimal evasive maneuver are that it produces a larger miss distance against an augmented proportional navigation missile than a proportional navigation one.

Acknowledgement—The authors are indebted to Dr S. Uehara, Director, Plans and Programs Department TRDI of the Japan Defense Agency, for giving us useful advice and discussing the paper.

REFERENCES

1. F. Imado and S. Miwa, The optimal evasive maneuver of a fighter against proportional navigation missiles. AIAA Paper 83-2139 (1983).
2. F. Imado and S. Miwa, Fighter evasive maneuvers against proportional navigation missile. *J. Aircraft* **23**, 825–830 (1986).
3. F. Imado and S. Miwa, Three dimensional study of evasive maneuvers of a fighter against a missile. AIAA Paper 86-2038 (1986).
4. F. W. Nesline and P. Zarchan, A new look at classical versus modern homing missile guidance. *J. Guid. Control* **4**, 78–85 (1981).
5. S. Akishita and F. Imado, General purpose tactical missile simulation program. *Proc. 13th A. Simulation Symp. Soc. Computer Simulation*, Tampa, Fla, March 1980, pp. 257–270 (1980).
6. A. E. Bryson Jr and W. F. Denham, A steepest ascent method for solving optimum programing problems. *J. appl. Méc.* **29**, 247–257 (1962).
7. A. E. Bryson Jr. and Y. C. Ho, *Applied Optimal Control*, pp. 221–228. Ginn-Blaisdell, Waltham, Mass (1969).
8. A. E. Bryson Jr and Y. C. Ho, *Applied Optimal Control*, pp. 154–155. Ginn-Blaisdell, Waltham, Mass (1969).
9. V. Garver, Optimum intercept laws for accelerating targets. *AIAA J.* **6**, 2196–2198 (1968).
10. R. K. Heffley and W. F. Jewell, Aircraft handling qualities data. NASA CR-2144, 61–107 (1972).
11. W. P. Gilbert, L. T. Nguyen and R. W. Van Gust, Simulation study of the effectiveness of an automatic control system designed to improve the high-angle-of-attack characteristics of a fighter airplane. NASA TN D-8176 (1976).